

# Flexural vibrations of microcantilevers coupled with a nanofiber

Philip A Yuya and Joseph A Turner<sup>1</sup>

Department of Engineering Mechanics, University of Nebraska-Lincoln, NE 68588-0526, USA

E-mail: [jaturner@unl.edu](mailto:jaturner@unl.edu)

Received 30 June 2007, in final form 14 August 2007

Published 11 September 2007

Online at [stacks.iop.org/Nano/18/405502](http://stacks.iop.org/Nano/18/405502)

## Abstract

In this study, the flexural vibrations of a microcantilever system coupled with a nanofiber offset from the free ends of the cantilevers are explored. Here, for this system, we derive the general expressions for the characteristic equation and sensitivity of vibration modes of a microcantilever system with a nanofiber wrapped offset from the free ends of the cantilevers. It is shown that each mode has a different sensitivity that depends on the nanofiber stiffness relative to the beam stiffness. We also show how the characteristic equation can be exploited with the knowledge of the resonant frequencies to determine the nanofiber stiffness and its attachment position on the microcantilevers. Plots of nanofiber position on the cantilevers versus wavenumber are used to show the effect of the position of the nanofiber on frequency measurements. The results are anticipated to provide a basic understanding between the vibration modes and the properties of the electrospun nanofibers, that may be used to optimize the experiments.

## 1. Introduction

The advantages of nanomaterials manufactured from continuous nanofibers obtained through the electrospinning process have been extensively discussed in the literature [1–6]. Due to their small size, the nanofiber diameters preclude the use of conventional techniques for characterizing their mechanical properties. Several nanomechanical characterization techniques have been suggested by many researchers [7–14]. Vibrations excited by thermal or electrical loads have been used to measure elastic properties of carbon nanotubes [15–18]. Simplification of the acoustical vibrations of atomic force microscope cantilevers has been successful in materials property characterization at the nanoscale level [19]. In our previous study, it was shown that one such technique involves the vibrations of two microcantilevers with a nanofiber wrapped on them [20]. This technique utilizes the dynamic response of the coupled microcantilever beams. A grounded metal tweezers is utilized to ‘capture’ a single nanofiber during electrospinning by placing the tweezers aside the electrospinning jet instability zone [21]. The single nanofiber spun on the tweezers is then

transported and suspended between two AFM cantilevers and the ends wrapped around the cantilevers. The frequencies of the cantilever resonances are recorded for both the free cantilever vibrations and for the case where the microcantilever system has nanofibers attached. The Young’s modulus is calculated from the resonant frequency shift resulting from the nanofiber.

The sensitivity of vibration modes of a beam in flexural vibrations, which is a measure of the relative change in frequency of a mode due to changes in nanofiber stiffness, is of much interest since each mode has different sensitivity to the variations in the nanofiber stiffness. It has been shown that the vibration modes of atomic force microscope (AFM) microcantilevers in surface contact are sensitive to surface stiffness variations [22–24]. The position of the nanofiber on the cantilevers also affects the frequency shift. For example, nanofibers attached close to the clamped end will have no significant effect on the resonances of the system. Both of these aspects are addressed here.

In this paper, the expressions that yield the general form of the characteristic equation and modal sensitivity of the microcantilever beams with a wrapped nanofiber offset from the free ends of the cantilevers are derived. It is also shown

<sup>1</sup> Author to whom any correspondence should be addressed.

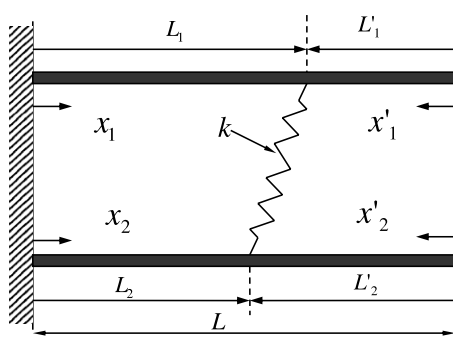


**Figure 1.** Schematic of the problem showing two prismatic beams cantilevered at one end and coupled with a nanofiber of stiffness  $k$  offset from the ends of the cantilevers.

how the characteristic equation of the system can be exploited, using frequency information, to determine the stiffness of the nanofiber. This aspect eliminates the need for scanning electron microscope (SEM) and finite element method (FEM) used in our previous work [20].

## 2. Theoretical model

Consider two identical microcantilevers coupled by a single nanofiber as shown schematically in figure 1. The nanofiber is modeled as a linear spring with coupling that is assumed pinned. The boundary value problem (BVP) for the system has governing equations given by [20, 25, 26]

$$EIq_i''''(x, t) + A\rho\ddot{q}_i(x, t) = 0, \quad (i = 1, 2). \quad (1)$$

The cantilevers are divided into two parts  $L_i$  and  $L'_i$  ( $i = 1, 2$ ), with separate solutions  $q_i(x_i, t) = \Psi_i(x_i)e^{i\omega t}$  and  $q'_i(x'_i, t) = \Omega_i(x'_i)e^{i\omega t}$ , respectively. For the  $L_i$  sections of the beam, the boundary conditions at  $x_i = 0$  are  $\Psi_i(0) = 0$ ,  $\Psi'_i(0) = 0$ , which correspond to conditions of zero displacement and zero slope at the fixed end, respectively. For the  $L'_i$  sections, the boundary conditions at  $x'_i = 0$  are  $\Omega''_i(0) = 0$ ,  $\Omega'''_i(0) = 0$ , which corresponds to zero moment and shear force at the free ends of the cantilevers. The continuity conditions at  $x_i = L_i$  and  $x'_i = L'_i$  are given by

$$\Psi_i(L_i) = \Omega_i(L'_i), \quad (2)$$

$$\frac{\partial \Psi_i(L_i)}{\partial x_i} = -\frac{\partial \Omega_i(L'_i)}{\partial x'_i}, \quad (3)$$

$$\frac{\partial^2 \Psi_i(L_i)}{\partial x_i^2} = \frac{\partial^2 \Omega_i(L'_i)}{\partial x_i'^2}, \quad (4)$$

$$-EI \frac{\partial^3 \Psi_1(L_1)}{\partial x_1^3} = EI \frac{\partial^3 \Omega_1(L'_1)}{\partial x_1'^3} - k[\Psi_1(L_1) - \Psi_2(L_2)], \quad (5)$$

$$-EI \frac{\partial^3 \Psi_2(L_2)}{\partial x_2^3} = EI \frac{\partial^3 \Omega_2(L'_2)}{\partial x_2'^3} + k[\Psi_1(L_1) - \Psi_2(L_2)]. \quad (6)$$

At the point of continuity, the cantilever displacement, slope and bending moments are equal as shown in equations (2)–(4) respectively. Equations (5) and (6) show that the difference of the shear forces exerted by the two sections of the cantilever

beams is carried by the nanofiber. The difference in the beam lengths  $L_1$  and  $L_2$  is assumed small enough to enable a small angle approximation for simplification of the problem. If the difference in length is significantly large, then the last term in equations (5) and (6) should be multiplied by  $\cos \theta$ , where  $\theta$  is the angle between the nanofiber and the outward normal of the microcantilever beams. However, such a geometry may be problematic experimentally due to the enhanced potential for nanofiber buckling. The transcendental characteristic function  $C(\gamma, \eta)$  (derived in the appendix), is obtained by equating the determinant of  $\underline{\underline{S}}$  to zero. It can be solved numerically for the values of the wavenumbers of the system. If  $L_1 = L_2$ , a case where the fiber is perpendicular to both beams, the characteristic function  $C(\gamma, \eta)$  which depends on the dimensionless wavenumber  $\gamma = \lambda L_1$  and stiffness ratio  $\eta = k/k_c$ , ( $k_c = 3EI/L^3$  is the stiffness of the beam), can be expressed in terms of a length ratio  $R = L_1/L$ . When  $R = 1$ , the characteristic equation simplifies to  $\{\gamma^3(1 + \cos \gamma \cosh \gamma) - 2\eta(\cos \gamma \sinh \gamma - \sin \gamma \cosh \gamma)\}\{\gamma^3(1 + \cos \gamma \cosh \gamma)\} = 0$ , which is the result for the case where the nanofiber is wrapped at the ends of the two cantilevers [20]. Next, the modal sensitivity of this problem is considered.

## 3. Modal sensitivity

The frequency difference between free resonance of the cantilever and the resonance of the microcantilever system with the attached nanofiber depends on the vibration modes. Different modes have different sensitivity to the stiffness of the nanofiber. The vibration modes that are most sensitive to the nanofiber stiffness are of interest when selecting the cantilevers. From the characteristic function  $C(\gamma, \eta)$ , the interest lies in the change of  $\gamma$  with respect to  $\eta$ . Differentiating  $C(\gamma, \eta)$  with respect to  $\eta$  implies that  $dC(\gamma, \eta)/d\eta = 0$ :

$$\frac{\partial C(\gamma, \eta)}{\partial \eta} + \frac{\partial C(\gamma, \eta)}{\partial \gamma} \frac{d\gamma}{d\eta} = 0, \quad (7)$$

from which the wavenumber sensitivity to changes in nanofiber stiffness is given by

$$\frac{d\gamma}{d\eta} = -\frac{\partial C/\partial \eta}{\partial C/\partial \gamma}. \quad (8)$$

From experiments, it is the change in frequency that is measured. Therefore, the change in frequency with respect to stiffness ratio is expressed as

$$\frac{\partial f}{\partial \eta} = \frac{\partial f}{\partial \gamma} \frac{d\gamma}{d\eta}. \quad (9)$$

The relationship between the wavenumber and frequency is given by  $f = (\gamma^2 \sqrt{EI/A\rho})/2\pi L^2$ . Differentiating  $f$  with respect to  $\gamma$  gives

$$\frac{\partial f}{\partial \gamma} = \frac{\gamma}{\pi} \sqrt{\frac{EI}{A\rho L^4}}. \quad (10)$$

By making use of equations (8)–(10) the change in frequency relative to nanofiber stiffness can therefore be expressed as

$$\frac{df}{d\eta} = -\frac{\partial C/\partial \eta}{\partial C/\partial \gamma} \frac{\gamma}{\pi} \sqrt{\frac{EI}{A\rho L^4}}. \quad (11)$$

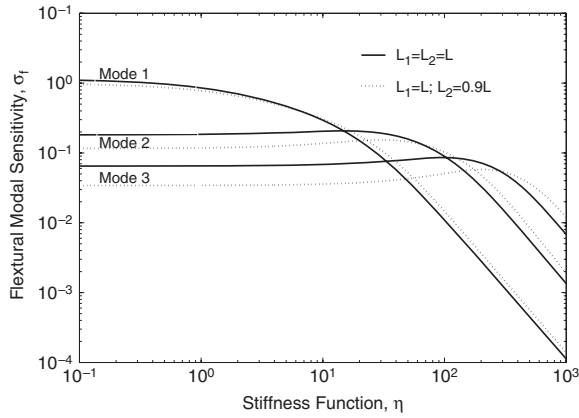


**Figure 2.** Normalized flexural modal sensitivity (equation (12)) of a rectangular cantilever as a function of normal nanofiber stiffness showing the first three modes.

Equation (11) can be normalized as

$$\sigma_f = \left( \frac{df}{d\eta} \right) \left( \frac{1}{2\pi} \sqrt{\frac{EI}{A\rho L^4}} \right)^{-1} = -2\gamma \frac{\partial C / \partial \eta}{\partial C / \partial \gamma}, \quad (12)$$

which is the ratio of the frequency measurement resolution,  $df/d\eta$ , relative to the characteristic frequency for the cantilever,  $\frac{1}{2\pi} \sqrt{\frac{EI}{A\rho L^4}}$ . The flexural sensitivity,  $\sigma_f$ , of the first three modes is plotted in figure 2 for the case when the nanofiber is at the end of the two prismatic cantilever beams ( $L_1 = L_2 = L$ ) and for an angled nanofiber ( $L_1 = L$ ;  $L_2 = 0.9L$ ). In general, the sensitivity of the modes decreases with the mode number. However, for a nanofiber that is stiff relative to the beam stiffness, there are threshold values for  $\eta$  for which the sensitivity of the higher mode to changes in  $\eta$  is larger than the lower mode.

From the characteristic function  $C(\gamma, \eta)$ , the wavenumber, and hence frequency, varies with the nanofiber position,  $R = L_1/L$ , on the cantilevers. The relation of the wavenumber and the nanofiber position for stiffness ratio  $\eta = 30$  is shown in figure 3. As the value of  $R$  increases, the wavenumbers are observed to increase until a certain critical position where the wavenumbers are seen to have maxima. These critical nanofiber positions where maximum frequencies are experienced vary from one mode to the other. For the first mode, the critical nanofiber position is at  $\sim 90\%$  of the length of the beam from the clamped end where maximum frequency is experienced. For higher modes, there are very slight variations in the wavenumber values, which implies that the presence of nanofibers affects the first frequency but higher frequencies are not significantly affected. For very small values of  $R$ , the frequencies approach that of a beam in free vibration which indicates that nanofibers wrapped very close to the fixed end of the cantilevers have no significant effect on the frequencies as expected.

#### 4. Determination of nanofiber stiffness

In the previous study [20], a scanning electron microscope (SEM) was needed to determine the exact position of the

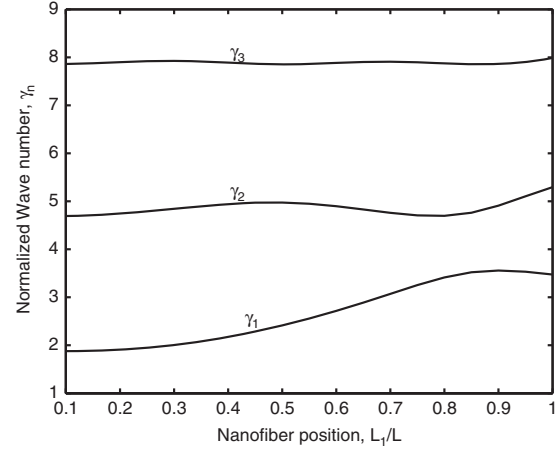


**Figure 3.** Relation between the nanofiber position  $R = L_1/L$  and wavenumber for modes 1, 2, and 3 for stiffness ratio  $\eta = 30$ .

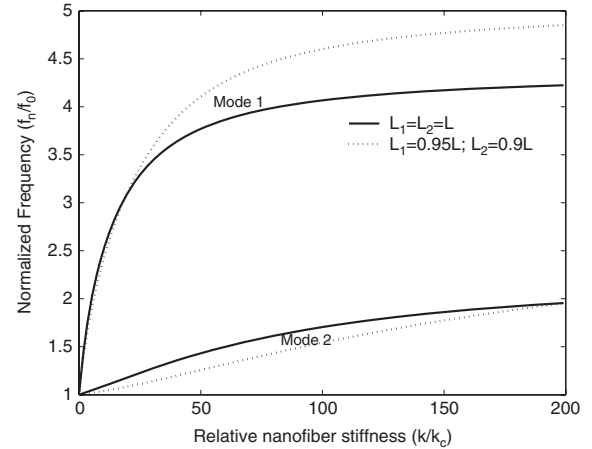


**Figure 4.** Flexural vibration frequency as a function of relative nanofiber stiffness for a microcantilever system coupled with a nanofiber.

nanofiber on the microcantilever beams. Also, the vibration analysis was done using the finite element method (FEM) to determine the nanofiber stiffness. Here, we detail how the nanofiber stiffness can be obtained without the need of either SEM or FEM. The stiffness of the nanofiber can be obtained from the flexural vibration frequency spectra of the microcantilever–nanofiber system. Stiffness curves as a function of frequency increment can be obtained for a particular cantilever type. The difference between the resonant frequency of the beam without the nanofiber and that of the beam with the fiber attached is taken as the frequency increment. Using this model, curves of frequency increment are plotted for a rectangular cantilever beam as a function of relative fiber stiffness. Figure 4 shows the normalized frequency as a function of relative nanofiber stiffness for the first and the second flexural modes for a rectangular beam system with the nanofiber wrapped at the end. Results such as these are used when selecting the cantilevers that are most sensitive to the nanofiber stiffness to maximize frequency response by estimating the expected values of the relative stiffness that will be obtained experimentally. It is evident from

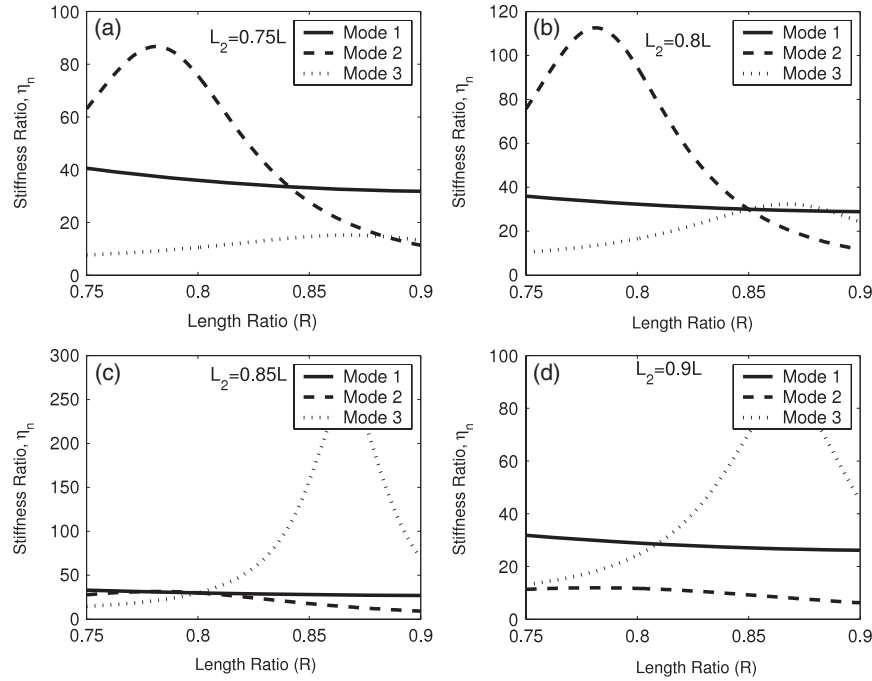


**Figure 5.** Results of  $\eta$  showing the procedure of self-consistent solution by variation of  $R$ . In this case, the relative nanofiber stiffness  $\eta = 30$  and the nanofiber is attached at  $L_1 = 0.8L$  and  $L_2 = 0.85L$ . The curves for the three modes intersect at one point giving values for  $\eta$  and  $R$  as shown in (b) and (c). In (a) and (d), where incorrect lengths are used, the points do not intersect.

figure 4 that the frequency depends on the nanofiber stiffness such that for very low values of stiffness ratio, the frequencies are close to those of a beam vibrating freely, while for very high values of the stiffness ratio, the frequencies approach those of a beam with pinned boundary conditions.

A characteristic beam constant  $C_B$ , relating the Young's modulus  $E$ , mass density  $\rho$  and the dimensions of the cantilever, can be obtained from the definition of the wavenumber as [27]

$$C_B^2 = \sqrt{4\pi^2 \frac{\rho A}{EI}} = \frac{\lambda_n^2}{f_n}, \quad (13)$$

where  $\lambda_n$  is the wavenumber and  $f_n$  is the frequency. The eigenvalue can then be expressed as

$$\lambda_n L_1 = C_B L_1 \sqrt{f_n}. \quad (14)$$

The characteristic function  $C(\gamma, \eta)$  is defined in terms of the length ratio  $R$  and can be solved numerically for  $\eta$  in terms of  $R$  by calculating  $\lambda_n L_1$  from the measured resonant frequencies. The measured free resonant frequencies along with the known values of  $\lambda_n L$  (i.e. 1.875, 4.694, 7.854, etc., for the free cases), which are roots of  $1 + \cos(\lambda_n L) \cosh(\lambda_n L) = 0$ , are used to calculate  $C_B$  since it is difficult to measure directly cantilever properties such as  $E$  and  $\rho$  and cross-sectional area  $A$ . The measured resonant frequency spectra with the nanofiber wrapped onto the cantilevers are used along with  $C_B L_1$  to calculate the new values for  $\lambda_n L_1$ , use being made of equation (14). The new values of  $\lambda_n L_1$  are then substituted back into the characteristic function  $C(\gamma, \eta)$  and solved to determine  $\eta$  as a function of  $R$  for each flexural mode. A plot of  $\eta$  versus  $R$  is obtained and the value of  $R$  for which all the

resonant modes intersect at the same point is considered as the correct solution for  $\eta$ . The stiffness ratio  $\eta$  must be the same for all cantilever vibration modes for a given measurement where the nanofiber position is located.

If the nanofiber is at a slight angle, three modes can be used to obtain the exact nanofiber position and stiffness as illustrated in figures 5 and 6. In figure 5, the first three wavenumbers for a nanofiber of a relative stiffness of 30, attached to the cantilevers at lengths  $L_1 = 0.85L$  and  $L_2 = 0.8L$  were obtained as 3.4702, 4.7294 and 7.8655, respectively. One length of the beams was fixed at the approximate position range while varying the other length as the wavenumbers were substituted back into the expression for the characteristic equation. Curves of stiffness ratio versus length ratio were plotted for all three modes. All the curves crossed at the point giving the values for the stiffness ratio and exact position of the nanofiber as shown in figure 5. However, for a value of  $L_1 \neq 0.85L$ , the curves do not intersect at a common point. In addition, it should be noted that the symmetry of the problem allows for two identical solutions for nanofiber position.  $L_1 = 0.8L$  also gives a solution to the problem since the two beams have the same properties and dimensions. Another example, shown in figure 6 for a nanofiber of stiffness ratio 10, positioned at  $L_1 = 0.95$  and  $L_2 = 0.9L$  with corresponding wavenumbers of 2.9086, 4.7851 and 7.8636, respectively, is illustrated in figure 6. If the two microcantilever beams are non-identical (i.e. variations in either dimensions or properties), then the symmetry depicted in figures 5 and 6 cannot be achieved. However, for slight variations, the intersection point can still be approximated. Experimentally, the nanofiber position can be approximated by measurements taken from a high-power optical microscope. A solution of

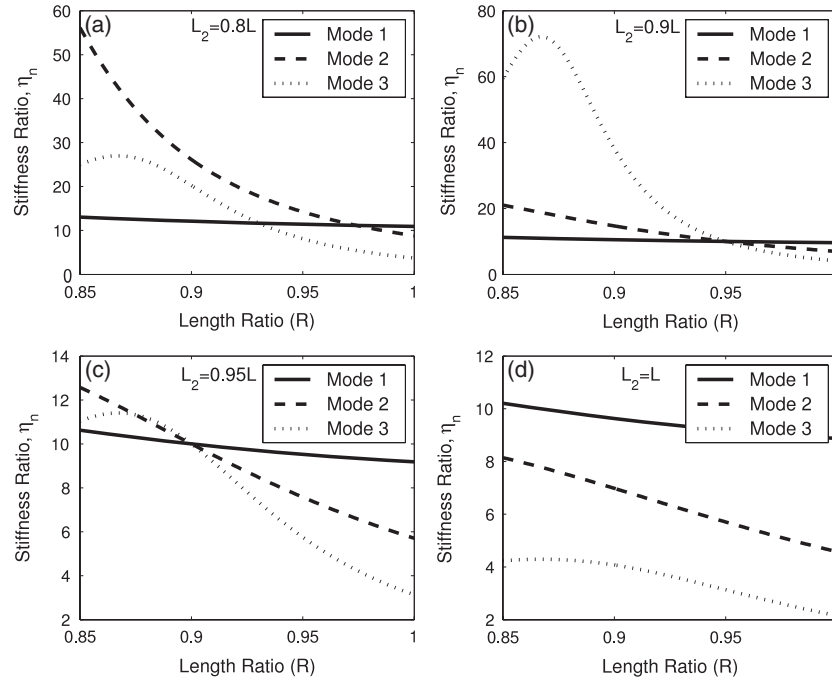


**Figure 6.** Results of  $\eta$  showing the procedure of self-consistent solution by variation of  $R$ . In this case, the relative nanofiber stiffness  $\eta = 30$  and the nanofiber is attached at  $L_1 = 0.95L$  and  $L_2 = 0.90L$ . The curves for the three modes intersect at one point giving values for  $\eta$  and  $R$  as shown in (b) and (c). In (a) and (d), where incorrect lengths are used, the points do not intersect.

the characteristic equation is then determined numerically by considering a small range of  $R$ . These illustrations show how measurements of the free resonant frequencies and resonant frequencies with nanofiber attached on the cantilevers can be used to determine the nanofiber stiffness.

## 5. Summary

In this paper, the vibrations of two microcantilevers coupled with a single nanofiber were examined. A linear spring has been used to model the nanofiber and the equations governing the flexural vibration modes for the case where two microcantilevers coupled with a nanofiber offset from the free ends were derived. The sensitivities of the modes to nanofiber stiffness have also been examined. It was shown that the first mode is the most sensitive for nanofibers that are stiff relative to the beam stiffness. It has also been shown how the characteristic equation can be used to determine the nanofiber stiffness by making use of both the uncoupled resonant frequency spectra and those of the system with the nanofiber wrapped on it. In principle, if the approximate position of the nanofiber on the microcantilever is known, three resonant frequency modes can be obtained experimentally and used to perform iterations to generate plots from which the stiffness information is obtained at the point where the three modes intersect. The major advantage of the microcantilever method is that it allows the mechanical properties of long free standing nanofibers to be determined.

In general, the sensitivity of the modes has been shown to decrease with the mode number for the system in flexural vibration. However, when the stiffness ratio is high enough, there are threshold values above which the higher-order modes

are more sensitive than the lower modes. The wavenumber of the system also varies with the distance of the nanofiber from the fixed end. The position of the nanofiber on the cantilever has an effect on the frequency measurements such that, if the nanofiber is very close to the fixed end, the wavenumber values approach those of a beam in free vibration, meaning that there is no significant difference in frequency measurements. This work is anticipated to contribute towards the research and development of continuous nanofibers with well-controlled mechanical and functional properties which can be used in the manufacture of nanofiber-based structures and devices.

## Acknowledgment

This work was supported by the National Science Foundation under grant no. DMI-0210850.

## Appendix

To aid in the solution of the eigenvalue problem (EVP) that results from simplification of equation (1), the general solution for  $\Psi_i(x_i)$  and  $\Omega_i(x'_i)$  can be written in the following form, shown here for  $\Psi_i(x_i)$ :

$$\begin{aligned} \Psi_i(x_i) = & A_i(\cos(\lambda x_i) + \cosh(\lambda x_i)) \\ & + B_i(\cos(\lambda x_i) - \cosh(\lambda x_i)) + C_i(\sin(\lambda x_i) + \sinh(\lambda x_i)) \\ & + D_i(\sin(\lambda x_i) - \sinh(\lambda x_i)), \quad (i = 1, 2) \end{aligned}$$

where  $\lambda^4 = (\frac{\rho A \omega^2}{EI})$  is the flexural wavenumber, with  $A_i$ ,  $B_i$ ,  $C_i$  and  $D_i$  as unknown coefficients. Inserting the general solutions for  $\Psi_i(x_i)$  and  $\Omega_i(x'_i)$  into the boundary and continuity conditions (equations (2)–(6)) and

performing algebraic manipulation leads to eight simultaneous homogeneous equations in terms of unknown coefficients  $J_i$ , ( $i = 1, \dots, 8$ ), where  $J_i$  are functions of  $A_i$ ,  $B_i$ ,  $C_i$  and  $D_i$ :

$$J_1\{\cos(\lambda L_1) - \cosh(\lambda L_1)\} + J_2\{\sin(\lambda L_1) - \sinh(\lambda L_1)\} - J_3\{\cos(\lambda L'_1) + \cosh(\lambda L'_1)\} - J_4\{\sin(\lambda L'_1) + \sinh(\lambda L'_1)\} = 0, \quad (15)$$

$$J_1\{\sin(\lambda L_1) + \sinh(\lambda L_1)\} + J_2\{\cos(\lambda L_1) - \cosh(\lambda L_1)\} - J_3\{\sin(\lambda L'_1) - \sinh(\lambda L'_1)\} + J_4\{\cos(\lambda L'_1) + \cosh(\lambda L'_1)\} = 0, \quad (16)$$

$$J_1\{\cos(\lambda L_1) + \cosh(\lambda L_1)\} - J_2\{\sin(\lambda L_1) + \sinh(\lambda L_1)\} + J_3\{\cos(\lambda L'_1) - \cosh(\lambda L'_1)\} + J_4\{\sin(\lambda L'_1) - \sinh(\lambda L'_1)\} = 0, \quad (17)$$

$$J_1\{-EI\lambda^3[\sin(\lambda L_1) - \sinh(\lambda L_1)] + k[\cos(\lambda L_1) - \cosh(\lambda L_1)] + J_2\{EI\lambda^3[\cos(\lambda L_1) + \cosh(\lambda L_1)] + k[\sin(\lambda L_1) - \sinh(\lambda L_1)] + J_3\{-EI\lambda^3[\sin(\lambda L'_1) + \sinh(\lambda L'_1)] + J_4\{EI\lambda^3[\cos(\lambda L'_1) - \cosh(\lambda L'_1)] + J_5\{-k[\cos(\lambda L_2) - \cosh(\lambda L_2)] + J_6\{-k[\sin(\lambda L_2) - \sinh(\lambda L_2)]\} = 0, \quad (18)$$

$$J_1\{-k[\cos(\lambda L_1) - \cosh(\lambda L_1)] + J_2\{-k[\sin(\lambda L_1) - \sinh(\lambda L_1)] + J_5\{-EI\lambda^3[\sin(\lambda L_2) - \sinh(\lambda L_2)] + k[\cos(\lambda L_2) - \cosh(\lambda L_2)] + J_6\{EI\lambda^3[\cos(\lambda L_2) + \cosh(\lambda L_2)] + k[\sin(\lambda L_2) - \sinh(\lambda L_2)] + J_7\{-EI\lambda^3[\sin(\lambda L'_2) + \sinh(\lambda L'_2)] + J_8\{EI\lambda^3[\cos(\lambda L'_2) - \cosh(\lambda L'_2)]\} = 0, \quad (19)$$

$$J_5\{\cos(\lambda L_2) + \cosh(\lambda L_2)\} - J_6\{\sin(\lambda L_2) + \sinh(\lambda L_2)\} + J_7\{\cos(\lambda L'_2) - \cosh(\lambda L'_2)\} + J_8\{\sin(\lambda L'_2) - \sinh(\lambda L'_2)\} = 0, \quad (20)$$

$$J_5\{\sin(\lambda L_2) + \sinh(\lambda L_2)\} + J_6\{\cos(\lambda L_2) - \cosh(\lambda L_2)\} - J_7\{\sin(\lambda L'_2) - \sinh(\lambda L'_2)\} + J_8\{\cos(\lambda L'_2) + \cosh(\lambda L'_2)\} = 0, \quad (21)$$

$$J_5\{\cos(\lambda L_2) - \cosh(\lambda L_2)\} + J_6\{\sin(\lambda L_2) - \sinh(\lambda L_2)\} - J_7\{\cos(\lambda L'_2) + \cosh(\lambda L'_2)\} - J_8\{\sin(\lambda L'_2) + \sinh(\lambda L'_2)\} = 0. \quad (22)$$

Equations (15)–(22) can be written as

$$\underline{\underline{S}}\underline{\underline{J}} = \underline{\underline{0}}. \quad (23)$$

Non-trivial solutions require  $C(\gamma, \eta) = 0$  from which the characteristic equation governing the allowable wavenumbers may be obtained. The characteristic function  $C(\gamma, \eta)$  is used in the main body of the paper.

## References

- [1] Dzenis Y 2004 Spinning continuous fibers for nanotechnology *Science* **304** 1917–9

- [2] Dzenis Y A and Wen Y 2001 Continuous carbon nanofibers for nanofiber composites *Proc. 2001 MRS Fall Mtg (Boston, Nov. 2001)* Paper 47481
- [3] Chew S Y, Wen Y, Dzenis Y and Leong K L 2006 The role of electrospinning in the emerging field of nanomedicine *Curr. Pharm. Des.* **12** 4751–70
- [4] Pan Z W, Xie S S, Lu L, Chang B H, Sun L F, Zhou W Y, Wang G and Zhang D L 1999 Tensile tests of ropes of very long aligned multiwall carbon nanotubes *Appl. Phys. Lett.* **74** 3152–4
- [5] Inai R, Kotaki M and Ramakrishna S 2005 Structure and properties of electrospun PLLA single nanofibers *Nanotechnology* **16** 208–13
- [6] Tan E P S and Lim C T 2004 Novel approach to tensile testing of micro- and nanoscale fibers *Rev. Sci. Instrum.* **75** 2581–5
- [7] Salvétat J P, Kulik A J, Bonard J M, Briggs G A D, Stockli T, Metenier K, Bonnamy S, Beguin F, Burnham N A and Forro L 1999 Elastic modulus of ordered and disordered multiwalled carbon nanotubes *Adv. Mater.* **11** 161–5
- [8] Walters A D, Ericson L M, Casavant M J, Liu J, Colbert D T, Smith K A and Smalley R E 1999 Elastic strain of freely suspended single-wall carbon nanotube ropes *Appl. Phys. Lett.* **74** 3803–5
- [9] Tombler T W, Chongwu Z, Alexseyev L, Jing K, Hongjie D, Lei L, Jayanthi C S, Meijie T and Wu S Y 2000 Reversible electromechanical characteristics of carbon nanotubes under local-probe manipulation *Nature* **405** 769–72
- [10] Paulo A S, Bokor J, Howe R T, He R, Yang P, Gao D, Carraro C and Maboudian R 2005 Mechanical elasticity of single and double clamped silicon nanobeams fabricated by the vapor–liquid–solid method *Appl. Phys. Lett.* **87** 053111
- [11] Tan E P S and Lim C T 2004 Physical properties of a single polymeric nanofiber *Appl. Phys. Lett.* **84** 1603–5
- [12] Bellan L M, Kameoka J and Craighead H G 2005 Measurement of the Young's moduli of individual polyethylene oxide and glass nanofibers *Nanotechnology* **16** 1095–9
- [13] Lee S H, Tekmen C and Sigmund W M 2005 Three-point bending of electrospun TiO<sub>2</sub> nanofibers *Mater. Sci. Eng. A* **398** 77–81
- [14] Gu S Y, Wu Q L, Ren J and Vancso G J 2005 Mechanical properties of a single electrospun fiber and its structures *Macromol. Rapid Commun.* **26** 716–20
- [15] Treacy M M J, Ebbesen T and Gibson J M 1996 Exceptionally high Young's modulus observed for individual carbon nanotubes *Nature* **381** 678–80
- [16] Poncharal P, Wang Z L, Ugarte D and de Heer W A 1999 Electrostatic deflections and electromechanical resonances of carbon nanotubes *Science* **283** 1513–6
- [17] Wang Z L, Poncharal P and de Heer W A 2000 Measuring physical and mechanical properties of individual carbon nanotubes by *in situ* TEM *J. Phys. Chem. Solids* **61** 1025–30
- [18] Wang Z L, Gao R P, Pan Z W and Dai Z R 2001 Nano-scale mechanics of nanotubes, nanowires, and nanobelts *Adv. Eng. Mater.* **3** 657–61
- [19] Rabe U, Turner J and Arnold W 1998 Analysis of the high-frequency response of atomic force microscope cantilevers *Appl. Phys. A* **66** S227–82
- [20] Yuya P A, Wen Y, Turner J A, Dzenis Y A and Li Z 2007 Determination of the Young's modulus of individual electrospun nanofibers by microcantilever vibration method *Appl. Phys. Lett.* **90** 111909
- [21] Reneker D H, Yarin A L, Fong H and Koombhongse S 2000 Bending instability of electrically charged liquid jets of polymer solutions in electrospinning *J. Appl. Phys.* **87** 4531–47
- [22] Turner J A and Wiehn J S 2001 Sensitivity of flexural and torsional vibration modes of atomic force microscope cantilevers to surface stiffness variations *Nanotechnology* **12** 322–9

- [23] Chang W J 2002 Sensitivity of vibration modes of atomic force cantilevers in continuous surface contact *Nanotechnology* **13** 510–4
- [24] Shen K, Hurley D C and Turner J A 2004 Dynamic behaviour of dagger-shaped cantilevers for atomic force microscopy *Nanotechnology* **15** 1582–9
- [25] Meirovitch L 1997 *Principles and Techniques of Vibrations* (Saddle River, NJ: Prentice-Hall) p 07458
- [26] Rabe U, Janser K and Arnold W 1996 Vibrations of free and surface-coupled atomic force microscope cantilevers: theory and experiment *Rev. Sci. Instrum.* **67** 3281
- [27] Rabe U, Amelio S, Kester E, Scherer V, Hirsekorn S and Arnold W 2000 Quantitative determination of contact stiffness using atomic force acoustic microscopy *Ultrasonics* **38** 430–7